

Chemical trends of magnetic interaction in Mn-doped III-V semiconductors

Haowei Peng, Jingbo Li, and Su-Huai Wei

Citation: *Appl. Phys. Lett.* **102**, 122409 (2013); doi: 10.1063/1.4799164

View online: <http://dx.doi.org/10.1063/1.4799164>

View Table of Contents: <http://apl.aip.org/resource/1/APPLAB/v102/i12>

Published by the [American Institute of Physics](#).

Additional information on Appl. Phys. Lett.



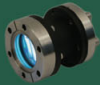



Journal Homepage: <http://apl.aip.org/>

Journal Information: http://apl.aip.org/about/about_the_journal

Top downloads: http://apl.aip.org/features/most_downloaded

Information for Authors: <http://apl.aip.org/authors>

ADVERTISEMENT

a sampling of our products		for surface and materials science	www. rbdinstruments .com	celebrating over 20 years of innovation
 deposition tools	 desorption systems	 sputter ion sources	 viewports	 usb picoammeters

Chemical trends of magnetic interaction in Mn-doped III-V semiconductors

Haowei Peng,¹ Jingbo Li,^{1,a)} and Su-Huai Wei²

¹State Key Laboratory for Superlattices and Microstructures, Institute of Semiconductors, Chinese Academy of Sciences, P. O. Box 912, Beijing 100083, People's Republic of China

²National Renewable Energy Laboratory, Golden, Colorado 80401, USA

(Received 28 December 2012; accepted 19 March 2013; published online 29 March 2013)

The trends of magnetic coupling strength in Mn-doped III-V semiconductors are explained using a physically transparent band-coupling model, based on first-principles calculations. According to this model, the stability of the ferromagnetism in Mn-doped III-V semiconductors should increase with both the strength of p - d coupling and an effective coupling range parameter, α . However, these two quantities counteract to each other, i.e., increased p - d coupling strength means a decreased α value. Therefore, this competition will lead to the non-monotonic variation of ferromagnetic interaction in Mn-doped common-cation III-V semiconductors as the anion becomes heavier. Our results suggest that Mn-doped GaAs and AlAs are optimal materials for high T_C spintronics, in good agreement with experimental observations. © 2013 American Institute of Physics. [<http://dx.doi.org/10.1063/1.4799164>]

Ferromagnetism in diluted magnetic semiconductors (DMSs) has been widely studied over the last decade. For Mn-doped III-V semiconductors, such as GaX:Mn (X = P, As, and Sb), Zener's model^{1,2} is usually used to explain their magnetic behavior. In GaX:Mn, divalent Mn, substituting for trivalent Ga, acts as both an acceptor to generate holes and a source of magnetic moments. According to Zener's model, the local moments on the Mn sites couple with each other via the help of the host valence p states, i.e., the so-called p - d coupling. Zener's model has predicted that the ferromagnetic (FM) transition temperature T_C increases with hole carrier density. In early empirical model calculations, it is suggested that T_C is higher in GaAs:Mn than in GaP:Mn and GaSb:Mn, given the same Mn and hole concentrations.^{1,3} However, a recent Monte Carlo study, which uses a different model Hamiltonian, reported a monotonic decrease of T_C from GaP:Mn to GaAs:Mn and then to GaSb:Mn.⁴ Experimentally, the highest T_C , 173 K, is observed in GaAs:Mn with 9% Mn content,^{5,6} which was improved to 200 K via nanostructure engineering.⁷ To further increase T_C , it is imperative to understand the origin of the chemical trends of the magnetic interactions in this Mn-doped III-V semiconductor system and whether GaAs is the best parent material for Mn-doped DMSs.

Despite great achievements in predicting the magnetic properties in DMSs, the phenomenological models are not transparent due to the various parameters used in the model Hamiltonians, and the reliability of the predictions also becomes questionable as demonstrated by the conflicting trends reported in Refs. 3 and 4. By contrast, the band coupling model,^{8,9} which has been proposed to explain the magnetic coupling in transition-metal-doped III-V and II-VI semiconductors, is based on first-principles calculations, where no empirical parameters are needed in principle and have been widely used in studying various properties of Mn-doped III-V semiconductors.¹⁰⁻¹² In this study, we will use the band-coupling model to investigate the trends of the stability of ferromagnetism in GaX:Mn and other III-V semiconductor systems.

The III-V semiconductors have the zincblende crystal structure with T_d symmetry. The valence band maximum (VBM) in GaX consists of mostly anion p orbitals, as well as some Ga $3d$. Under the T_d symmetry, the p orbitals form the triply degenerate t_{2p} state. When a Mn atom substitutes for Ga in GaX, the Mn $3d$ orbitals will split into t_{2d} and e_d states due to the tetrahedral crystal field. The t_{2d} state will couple strongly with the host t_{2p} states because of the same symmetry. In GaX:Mn, the host VBM t_{2p} state is sandwiched between the Mn spin-up and spin-down d states. Without spin-orbital interaction, only the states in the same spin channel will couple with each other. There are three types of important band coupling in this system: p - d coupling with t_{2p} above t_{2d} , p - d coupling with t_{2p} below t_{2d} , and d - d coupling between majority spin and minority spin t_{2d} states, with level-level repulsion energies of Δ_{pd}^1 , Δ_{pd}^2 , and $\Delta_{dd}^{1,2}$, respectively, as illustrated in the top panel of Fig. 1. The stability of ferromagnetism can be measured by the FM stabilization energy, ΔE_{AFM-FM} , which is defined by the energy difference between the antiferromagnetic (AFM) and FM phases. Based on the band-coupling model (see Fig. 1 and Refs. 8 and 9 for more details),

$$\Delta E_{AFM-FM} = \alpha m_h (\Delta_{pd}^1 + \Delta_{pd}^2) - 6\Delta_{dd}^{1,2}, \quad (1)$$

where m_h is the number of holes in the system (for GaX:Mn, each Mn on Ga site substitution creates one hole). The above equation shows that the magnetic ground state is determined by three factors: The first one is the strength of the p - d coupling, $\Delta_{pd} = \Delta_{pd}^1 + \Delta_{pd}^2$, which describes the spin-exchange splitting of the host p states due to the p - d coupling. The second factor is the effective coupling range parameter, α , which describe the extent of the p - d coupling. When the p orbital is fully delocalized, it will couple with all the Mn d orbitals in the cell equally, so its exchange splitting should depend linearly on Mn concentration with $\alpha = 1$. However, in reality, the p orbital will become localized due to the p - d coupling, so $\alpha < 1$, and decreases when the hole states become more localized or when the Mn-Mn distance increases. The last factor is the strength of d - d coupling, $\Delta_{dd}^{1,2}$.

^{a)}Electronic address: jbli@semi.ac.cn

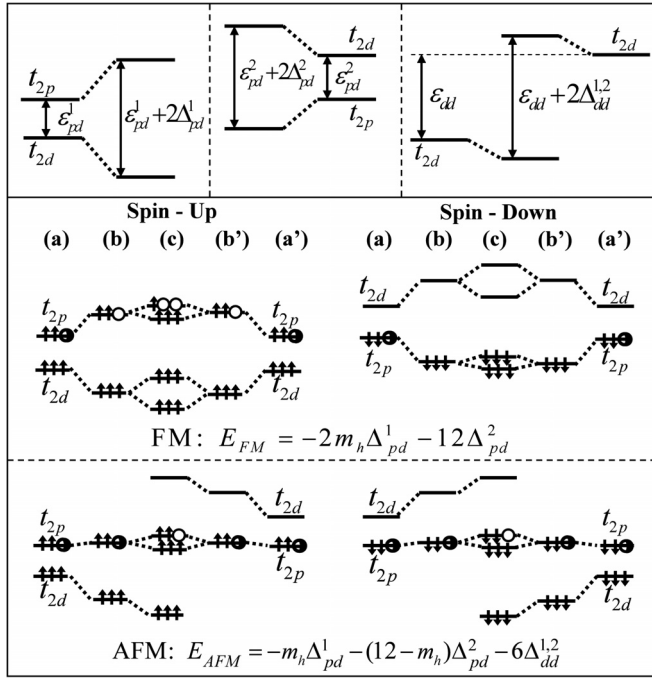


FIG. 1. Top panel: three types of band-coupling in GaX:Mn (X = P, As, and Sb). Bottom panel: the band coupling model^{8,9} for the FM and AFM phases of GaX:Mn. From (a) to (b) and (a') to (b'), only the p - d coupling is turned on. From (b) and (b') to (c), the d - d coupling is turned on. E_{FM} and E_{AFM} are the energy gain for the FM and AFM configurations, respectively. The FM stabilization energy is defined as $\Delta E_{AFM-FM} = E_{AFM} - E_{FM}$.

corresponds to the superexchange interaction,¹³ which stabilizes the AFM phase in Mn-doped III-V semiconductors.^{10,14} Due to the nature of an interaction between the localized metal d orbitals, $\Delta_{dd}^{1,2}$ is generally smaller than Δ_{pd} . So, the trend of the stability of the ferromagnetism in GaX:Mn can mainly be traced to the trends of the first two factors mentioned above, as the host changes from GaP to GaAs and then to GaSb.

To obtain these parameters, we have performed a series of band structure calculations using the first-principles method within the framework of density functional theory, as implemented in the VIENNA *AB INITIO* SIMULATION PACKAGE.¹⁵ The projected augmented wave¹⁶ (PAW) method is used to describe the electron-ion interaction, and the $3d$ electrons of Ga are treated as valence electrons. For the exchange-correlation potential, we choose the generalized gradient approximation (GGA) with the functional of Perdew, Burke, and Ernzerhof (PBE).¹⁷ To study the properties of substitutional Mn in GaX, we use the 64-atom supercells¹⁸ and compare the energies of FM and AFM phases in the supercells that contain up to two Mn atoms.¹⁰ A cutoff energy of 300 eV is used for the plane wave basis set, and a Γ -centered $4 \times 4 \times 4$ Monkhorst-Pack¹⁹ k -mesh is used for the Brillouin zone integration. For all the calculations, the atomic positions are relaxed until the Hellman-Feynman force is less than 0.01 eV/Å.

We first calculate the band structure of the pure host systems, and then we replace one Ga atom with Mn in the supercell. The parameters Δ_{pd}^1 and (Δ_{pd}^2) can be obtained by comparing the differences of the single-particle eigenvalues of the valence band edge states in the spin-up (spin-down) channel and the host VBM states. After that, the two nearest

neighboring (NN) Ga atoms are replaced by a pair of Mn atoms with their spin orientation parallel to each other (in the FM configuration). As shown in Fig. 1, the hole states in the spin-up channel are raised up by $2\alpha\Delta_{pd}^1$, which can be determined by the shift of the hole states with respect to the host VBM. Having the data of Δ_{pd}^1 and $2\alpha\Delta_{pd}^1$, the value of α can be derived. In this study, these three parameters are determined using the eigenvalues at the Γ point, as the symmetry is well defined at this point. To use a uniform reference energy in these supercell calculations, we align the atomic core levels of the atoms far from the Mn impurity sites. To calculate the FM stabilization energy, ΔE_{AFM-FM} , we also calculate the total energies for the AFM phase. In this case, we replace two NN Ga with a pair of Mn with their spin orientation antiparallel to each other. For systems studied in this paper, the NN interaction is dominant, so we focus only on the NN configuration. Finally, given the values of ΔE_{AFM-FM} , we can calculate $\Delta_{dd}^{1,2}$ using Eq. (1).

The calculated parameters Δ_{pd}^1 , Δ_{pd}^2 , α , $\Delta_{dd}^{1,2}$, and ΔE_{AFM-FM} for GaX:Mn systems are listed in Table I. In this system, we find Δ_{pd}^1 is much greater than Δ_{pd}^2 , so it is the main part in the p - d coupling. We see that when the anion changes from P to As and then to Sb, the coupling strengths Δ_{pd}^1 , Δ_{pd}^2 , and $\Delta_{dd}^{1,2}$ decrease. This is because when the anion atomic number increases from P to As and then to Sb, the lattice constant increases, and so do the Mn-X bond lengths, which tends to weaken the p - d coupling. Meanwhile, the separation between the Mn atoms also increases, which weakens the d - d coupling. Moreover, as the atomic number of the anion increases, the anion valence p orbital energies increase. Consequently, the host VBM t_{2p} state energy increases. So, as the anion changes from P to Sb, the energy difference between the host VBM t_{2p} states and the majority spin Mn t_{2d} states increases, which also weakens the p - d coupling according to the perturbation theory.

On the other hand, when the atomic number increases, the interaction range parameter α increases (Table I). This is because as the p - d coupling weakens with the increasing atomic number of the anions, the hybridized p - d coupling states become more delocalized. This trend is also reflected by the component of Mn- d states in the hole states at the Γ point, which indicates the mixing of the Mn- d states into the host VBM states. In GaP:Mn, GaAs:Mn, and GaSb:Mn systems, the component of Mn- d states in the hole states at Γ is 0.162, 0.116, and 0.056, respectively. The hole states with less d character are more delocalized. This can be seen clearly in Fig. 2, where we plot the charge density for the hole states at the Γ point in the $[110]$ plane of zinc-blende GaX:Mn. As expected, the α values increase when the hole state becomes more delocalized, in agreement with the band-coupling model.

TABLE I. The band-coupling model parameters for GaX:Mn systems. The unit for the energy terms is meV.

Host	Δ_{pd}^1	Δ_{pd}^2	α	$\Delta_{dd}^{1,2}$	ΔE_{AFM-FM}
GaP	411	87	0.795	95	221
GaAs	320	83	0.836	75	227
GaSb	220	83	0.885	64	150

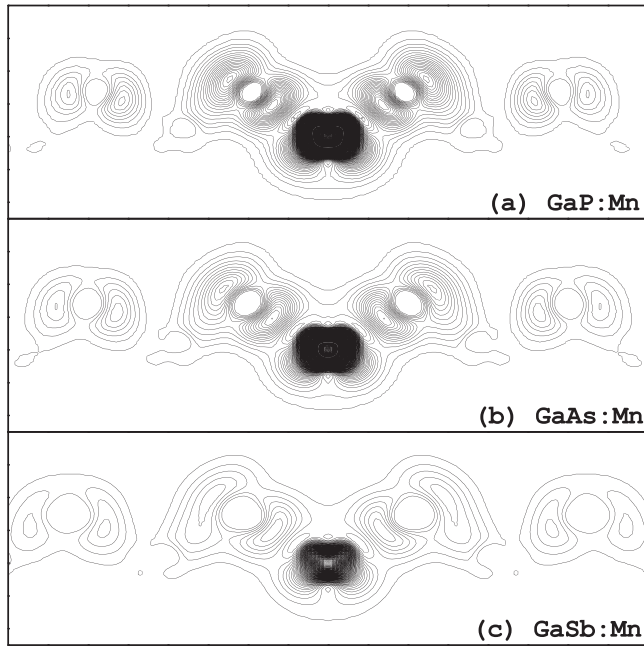


FIG. 2. Contour plot for the charge density of the hole states at the Γ point, in the $[110]$ plane of the zincblende structures (a) GaP:Mn, (b) GaAs:Mn, and (c) GaSb:Mn. The Mn atom is located at the center. The step size of the contours is $0.001 \text{ electron}/\text{\AA}^3$.

Because the FM stabilization energy is proportional to both Δ_{pd} and α , the opposite trends of Δ_{pd} and α can lead to a non-monotonic change in ΔE_{AFM-FM} , and we do find a maximum FM stabilization energy in GaAs:Mn.

As we have shown the trend of the stability of ferromagnetism in GaX:Mn systems and explained it with the band-coupling model, it will also be interesting to see whether these chemical trends also exist in other III-V semiconductors. To observe these trends, we perform similar calculations on AlX:Mn and InX:Mn systems. The calculated band-coupling model parameters and the FM stability energies are listed in Table II. On one hand, the trends of Δ_{pd}^1 , Δ_{pd}^2 , α , $\Delta_{dd}^{1,2}$, and ΔE_{AFM-FM} are very similar for AlX:Mn, GaX:Mn, and InX:Mn, as X changes from P to As and then to Sb. On the other hand, we also find that the p - d coupling becomes weaker as the cation changes from Al to Ga and then to In. The difference between Al compounds and Ga compounds, which have similar lattice constants, can be attributed to the p - d coupling between anion valence p states and the Ga $3d$ states. This p - d coupling in host materials raises the energies of host VBM states, which in turn reduces the coupling between the VBM t_{2p} and occupied Mn t_{2d} states. In AlX systems, there is no such p - d coupling because Al does not have occupied d states. For In compounds, the lattice constants are larger. This leads to a higher VBM energy and weak VBM t_{2p} and Mn t_{2d} coupling. As expected from the band-coupling model, we see that a small α always accompanies a strong p - d coupling.

In summary, via first-principles calculations, we study the stability of ferromagnetism in Mn-doped III-V semiconductors.

TABLE II. The band-coupling model parameters for AlX:Mn and InX:Mn systems.

Host	Δ_{pd}^1	Δ_{pd}^2	α	$\Delta_{dd}^{1,2}$	ΔE_{AFM-FM}
AlP	546	59	0.738	106	261
AlAs	419	53	0.780	75	285
AlSb	264	41	0.856	49	227
InP	337	73	0.816	80	188
InAs	259	73	0.852	62	194
InSb	190	64	0.861	51	131

Their chemical trends are explained with a band coupling model. It is the competition between the strength of the p - d coupling and an effective coupling range parameter α that results in the non-monotonic trend of the stability of ferromagnetism in these systems. As the host changes from GaP to GaAs and then to GaSb, the p - d coupling decreases (along with the d - d coupling, which is less important), while α increases. Thus, the maximum of the stability of ferromagnetism occurs in Mn-doped GaAs. Similar trends are also found in Mn-doped AlX:Mn and InX:Mn.

J. Li gratefully acknowledges financial support from the “One-Hundred Talents Plan” of the Chinese Academy of Sciences. The work at NREL was supported by the U.S. Department of Energy under Contract No. DE-AC36-08GO28308.

- ¹T. Dietl, H. Ohno, F. Matsukura, J. Cibert, and D. Ferrand, *Science* **287**, 1019 (2000).
- ²M. A. Scarpulla, B. L. Cardozo, R. Farshchi, W. M. Hlaing Oo, M. D. McCluskey, K. M. Yu, and O. D. Dubon, *Phys. Rev. Lett.* **95**, 207204 (2005).
- ³R. Bouzerar and G. Bouzerar, *Europhys. Lett.* **92**, 47006 (2010).
- ⁴Y. Yildirim, G. Alvarez, A. Moreo, and E. Dagotto, *Phys. Rev. Lett.* **99**, 057207 (2007).
- ⁵K. Y. Wang, R. P. Campion, K. W. Edmonds, M. Sawicki, T. Dietl, C. T. Foxon, and B. L. Gallagher, *AIP Conf. Proc.* **772**, 333 (2005).
- ⁶T. Jungwirth, K. Y. Wang, J. Masek, K. W. Edmonds, J. König, J. Sinova, M. Polini, N. A. Goncharuk, A. H. MacDonald, M. Sawicki, A. W. Rushforth, R. P. Campion, L. X. Zhao, C. T. Foxon, and B. L. Gallagher, *Phys. Rev. B* **72**, 165204 (2005).
- ⁷L. Chen, X. Yang, F. Yang, J. Zhao, J. Misuraca, P. Xiong, and S. von Molnár, *Nano Lett.* **11**, 2584 (2011).
- ⁸G. M. Dalpian, S.-H. Wei, X. G. Gong, A. J. R. da Silva, and A. Fazzio, *Solid State Commun.* **138**, 353 (2006).
- ⁹G. M. Dalpian and S.-H. Wei, *Phys. Status Solidi B* **243**, 2170 (2006).
- ¹⁰T. Jungwirth, J. Sinova, J. Mašek, J. Kušera, and A. H. MacDonald, *Rev. Mod. Phys.* **78**, 809 (2006) and references therein.
- ¹¹P. Mahadevan and A. Zunger, *Phys. Rev. B* **69**, 115211 (2004).
- ¹²P. Mahadevan and A. Zunger, *Appl. Phys. Lett.* **85**, 2860 (2004).
- ¹³P. W. Anderson, *Phys. Rev.* **79**, 350 (1950).
- ¹⁴J. B. Goodenough, *Phys. Rev.* **100**, 564 (1955); *J. Phys. Chem. Solids* **6**, 287 (1958); J. Kanamori, *J. Phys. Chem. Solids* **10**, 87 (1959).
- ¹⁵G. Kresse and D. Joubert, *Comput. Mater. Sci.* **6**, 15 (1996).
- ¹⁶G. Kresse and D. Joubert, *Phys. Rev. B* **59**, 1758 (1999).
- ¹⁷J. P. Perdew, K. Burke, and M. Ernzerhof, *Phys. Rev. Lett.* **77**, 3865 (1996).
- ¹⁸O. Madelung, *Semiconductors: Data Handbook*, 3rd ed. (Springer, Berlin, 2004).
- ¹⁹H. J. Monkhorst and J. D. Pack, *Phys. Rev. B* **13**, 5188 (1976).